Pediatric Radiology (2021) 51:1645–1653
https://doi.org/10.1007/s00247-021-05054-3

ORIGINAL ARTICLE

Free-breathing radial stack-of-stars three-dimensional Dixon gradient echo sequence in abdominal magnetic resonance imaging in sedated pediatric patients

Patrick B. Duffy[1] · Alto Stemmer[2] · Michael J. Callahan[1] · Joseph P. Cravero[3] · Patrick R. Johnston[1] · Simon K. Warfield[1] · Sarah D. Bixby[1]

Received: 30 November 2020 / Revised: 30 January 2021 / Accepted: 16 March 2021 / Published online: 8 April 2021

Abstract

Background There is a strong need for improvements in motion robust T1-weighted abdominal imaging sequences in children to enable high-quality, free-breathing imaging.

Objective To compare imaging time and quality of a radial stack-of-stars, free-breathing T1-weighted gradient echo acquisition (volumetric interpolated breath-hold examination [VIBE]) three-dimensional (3-D) Dixon sequence in sedated pediatric patients undergoing abdominal magnetic resonance imaging (MRI) against conventional Cartesian T1-weighed sequences.

Materials and methods This study was approved by the institutional review board with informed consent obtained from all subjects. Study subjects included 31 pediatric patients (19 male, 12 female; median age: 5 years; interquartile range: 5 years) undergoing abdominal MRI at 3 tesla with a free-breathing T1-weighted radial stack-of-stars 3-D VIBE Dixon prototype sequence, StarVIBE Dixon (radial technique), between October 2018 and June 2019 with previous abdominal MR imaging using conventional Cartesian T1-weighed imaging (traditional technique). MRI component times were recorded as well as the total number of non-contrast T1-weighted sequences. Two radiologists independently rated images for quality using a scale from 1 to 5 according to the following metrics: overall image quality, hepatic edge sharpness, hepatic vessel clarity and respiratory motion robustness. Scores were compared between the groups.

Results Mean T1-weighted imaging times for all subjects were 3.63 min for radial exams and 8.01 min for traditional exams (P<0.001), and total non-contrast imaging time was 32.7 min vs. 43.9 min (P=0.002). Adjusted mean total MRI time for all subjects was 60.2 min for radial exams and 65.7 min for traditional exams (P=0.387). The mean number of non-contrast T1-weighted sequences performed in radial MRI exams was 1.0 compared to 1.9 (range: 0–6) in traditional exams (P<0.001). StarVIBE Dixon outperformed Cartesian methods in all quality metrics. The mean overall image quality (scale 1–5) was 3.95 for radial exams and 3.31 for traditional exams (P<0.001).

Conclusion Radial stack-of-stars 3-D VIBE Dixon during free-breathing abdominal MRI in pediatric patients offers improved image quality compared to Cartesian T1-weighted imaging techniques with decreased T1-weighted and total non-contrast imaging time. This has important implications for children undergoing sedation for imaging.

Keywords Abdomen · Children · Free-breathing · Magnetic resonance imaging · Radial · Sedation · T1-weighted

✉ Sarah D. Bixby
sarah.bixby@childrens.harvard.edu

[1] Department of Radiology,
Boston Children's Hospital,
300 Longwood Ave., Boston, MA 02115, USA

[2] Siemens Healthineers,
Erlangen, Germany

[3] Department of Anesthesiology,
Boston Children's Hospital,
Boston, MA, USA

Introduction

Magnetic resonance imaging (MRI) is a commonly utilized modality for the evaluation of abdominopelvic disease in pediatric patients [1]. The most common indications for abdominal MRI in pediatric patients include diagnosis and staging of abdominal tumors and tumor-like lesions, and diagnosis of hepatobiliary conditions and genitourinary tract abnormalities [2]. T1-weighted gradient echo (GRE) imaging is a routine component of pediatric abdominal MRI [3]. Unenhanced

T1-weighted sequences aid in identifying and characterizing abdominal lesions, as well as in detecting hemorrhage or fat within lesions. In clinical practice, radiologists have relied on T1-weighted fast spin echo (FSE) or inversion recovery techniques with respiratory triggering or high NSA (number of signal averages) to reduce motion artifacts [1, 2, 4, 5] (Fig. 1). These techniques increase imaging time, and image quality depends greatly on the breathing pattern. With respiratory triggering, the contrast of each k-space readout may be inconsistent due to respiration-induced variation in timing. However, this compromise in image quality has been acceptable when the alternative is sedation or reacquisition. T1-weighted GRE techniques are faster, volumetric acquisitions that provide superior spatial resolution and anatomical detail than FSE sequences [6] and may be performed during a single breath-hold. In adults, a "comfortable" breath-hold is considered to be less than 25 s [7], though even a 15-s breath-hold may be too long for children [8]. Performing breath-hold imaging in sedated patients necessitates invasive airway management, which increases the potential risks of anesthesia. There is a strong need for improvements in motion robust T1-weighted imaging sequences. A navigated, free-breathing

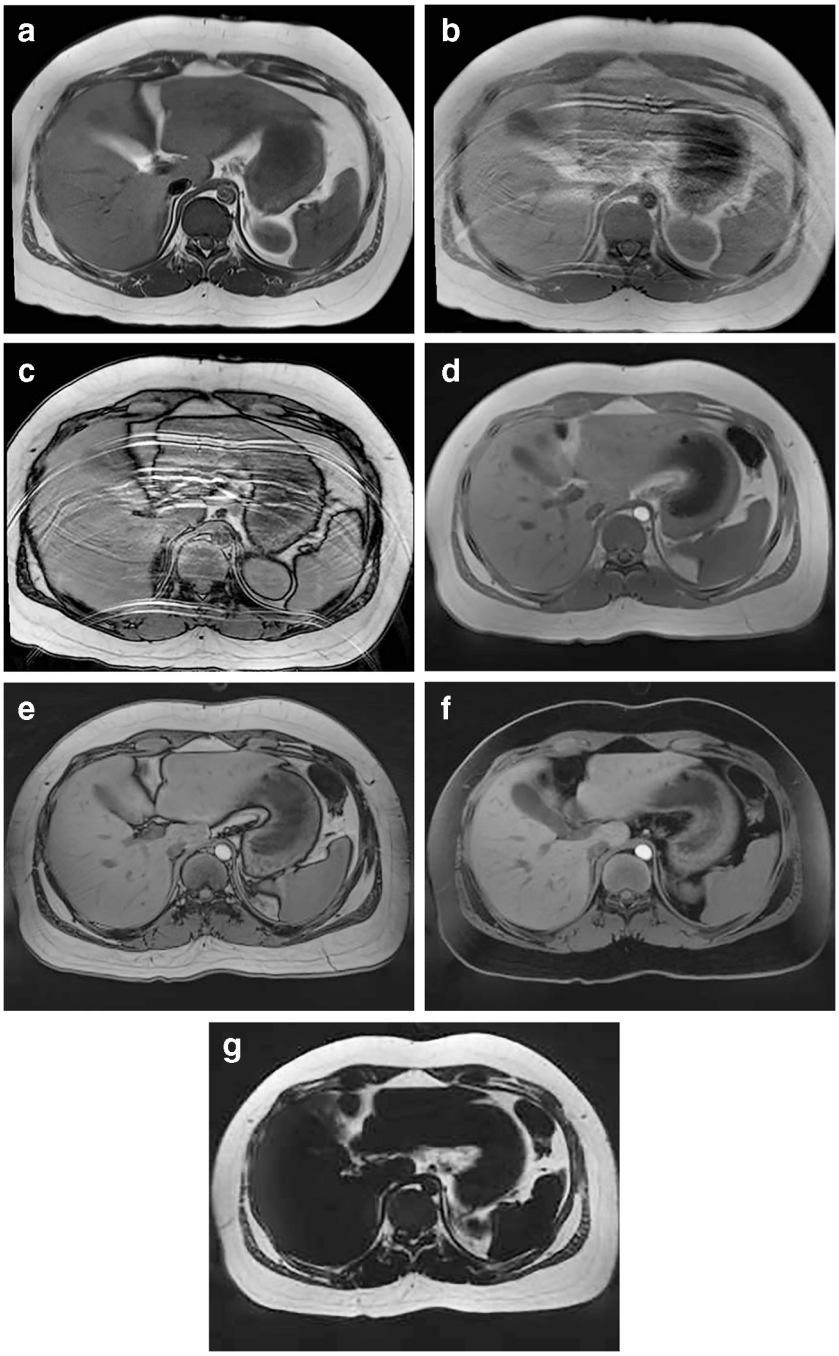

Fig. 1 A 14-year-old boy with tuberous sclerosis complex undergoing screening abdominal imaging. **a–c** A traditional MRI screening exam using an axial T1-weighted fast spin echo free-breathing sequence was performed with eight signal averages (**a**) along with axial gradient echo in-phase (**b**) and opposed-phase (**c**) imaging. Total T1 imaging time was 18 min and 6 s. The motion robustness score for the T1-weighted images was 3 from each reviewer (composite assessment of both sequences). **d–g** A radial exam performed on a Skyra scanner consisted of a free-breathing axial StarVIBE (volumetric interpolated breath-hold examination) Dixon. Total T1 imaging time was 2 min 14 s. Reader 1 gave an overall image quality score of 4 and reader 2 gave a score of 5

abdominal T1-weighted acquisition has been successfully applied in pediatric patients in the setting of post-contrast imaging [3], though it requires additional scan time and utilizes fat suppression, which makes it less useful for non-contrast imaging [3, 9]. A radial k-space sampling method for T1-weighted fat-suppressed, post-contrast GRE abdominal imaging in pediatric patients has demonstrated improved image quality and lesion conspicuity compared to the corresponding breath-held, Cartesian sequences [10–12].

T1-weighted abdominal imaging may be performed with in- and opposed-phase imaging to provide additional information about fat content, iron deposition or detection of lipid within lesions [13]. The Dixon method is a chemical shift imaging method that leverages the resonance frequencies of water and fat protons [14]. The StarVIBE Dixon sequence (Siemens Healthcare, Erlangen, Germany) is a two-point Dixon technique that provides a motion robust, free-breathing volumetric fat/water separation. This sequence acquires three-dimensional (3-D) multi-echo data with a radial stack-of-stars GRE sequence with bipolar readout. High-quality reconstructions can be obtained using a high readout bandwidth to reduce fat-water shift in a radial technique. In clinical practice, a single high-quality, free-breathing T1-weighted DIXON sequence substitutes up to three conventional, Cartesian T1-weighted sequences including spin echo sequences with and without fat suppression, and in- and opposed-phase GRE images (Fig. 1). Furthermore, non-Cartesian radial k-space sampling techniques offer motion-resistant alternatives to more conventional Cartesian acquisitions, which have been shown to decrease scan time in pediatric patients with tuberous sclerosis complex [13].

The purpose of this study was to compare the performance in terms of imaging time and image quality of a free-breathing, radial k-space gradient-echo Dixon technique (radial exam) in abdominal imaging in sedated pediatric patients to a traditional free-breathing protocol relying on either signal averaging or respiratory triggering of Cartesian T1-weighted pulse sequences (traditional exam).

Materials and methods

Patient selection

This was an institutional review board (IRB)-approved, Health Insurance Portability and Accountability Act (HIPAA)-compliant, single-center study. Eligible study subjects included patients ages newborn to 20 years who underwent abdominal MRI under sedation on a 3-tesla (T) magnet (MAGNETOM Skyra, Prisma or Trio; Siemens Healthcare) between October 2018 and June 2019 with a prototype StarVIBE Dixon sequence. Subjects were enrolled prospectively at the time of imaging and they and/or their guardian provided written, informed consent. Sedated patients were selected given their inability to breath-hold without invasive airway placement. After enrollment, some subjects were excluded because they had not undergone previous (within 3 years) 3-T abdominal MRI using traditional department protocols. The new and previous MRI exams for each patient will be referred to as the radial and traditional exams, respectively. Electronic medical records were reviewed to determine the clinical indication for each examination and patient demographics. Anesthesia records were reviewed to determine the mechanism of airway management (natural airway, laryngeal mask airway, endotracheal tube).

Imaging protocols

Imaging protocols were based on study indication (abdominal mass, liver mass, tuberous sclerosis, renal mass, fungemia). A 30-channel body matrix coil was used for patients scanned on the Prisma or Skyra magnets, and an 8-channel body coil was used for patients scanned on the Trio. Patients were breathing freely throughout both radial and traditional protocols. Individual sequence parameters for non-contrast T1-weighted images are listed in Table 1. All radial exams included a StarVIBE Dixon sequence, while all traditional exams included either a T1-weighted FSE sequence only (68%, 21/31), in- and opposed-phase GRE sequence only (16%, 5/31), or both (16%, 5/31).

The radial stack-of-stars StarVIBE Dixon sequence is an extension of the StarVIBE product sequence and was distributed by Siemens as a work in progress (WIP991B). The sequence is performed without navigation, and imaging parameters were selected to minimize off-resonance effects arising from fat while maintaining high spatial resolution across the abdomen (Table 1). In our study, the StarVIBE Dixon prototype was substituted for the standard T1-weighted sequences in abdominal MRI protocols in patients undergoing sedated abdominal MRI after obtaining written informed consent.

Of the 31 study subjects, 18 underwent imaging of multiple body parts under the same episode of anesthesia (e.g., abdomen MRI and one other body part). A cohort of patients was identified that shared three common factors between radial and traditional exams: (1) same body parts imaged in both imaging episodes (either abdomen only or abdomen + same additional body part), (2) same use/non-use of diffusion-weighted imaging sequences, and (3) same use/non-use of intravenous contrast and post-contrast imaging. This cohort comprised 13 subjects, which we labeled the "BDI" cohort (indicating the same status for body parts imaged, diffusion-weighted imaging, and intravenous contrast administration).

Table 1 Sequence parameters for T1-weighted non-contrast imaging for abdominal MRI protocols

Sequence description	Trajectory	TR/TE/TI (ms)	NSA	Flip angle (°)	Voxel size (mm)	Acceleration factor (GRAPPA)	Bandwidth (Hz/Px)	Radial views
Radial exam								
Axial T1-weighted StarVIBE Dixon	Radial	3.8/1.32 and 2.62	1	9	1.0×1.0×3.0	NA	1,200	980
Traditional exam								
Axial T1-weighted FSE	Cartesian	610/22	8	120	0.5×0.5×4.0	3	240	NA
Axial T1-weighted in and opposed phase	Cartesian	170/1.26 and 2.52	9	48	0.6×0.6×4.0	2	1,090	NA

FSE fast spin echo, *GRAPPA* generalized autocalibrating partial parallel acquisition, *NA* not applicable, *NSA* number of signal averages, *Px* pixel, *TE* echo time, *TI* inversion time, *TR* repetition time, *VIBE* volumetric interpolated breath-hold examination

Acquisition data

The DICOM (Digital Imaging and Communications in Medicine) data files for each MRI examination were reviewed and the following data were recorded: start time of the initial localizer sequence, end time of the final non-contrast sequence, end time of the final sequence, start and end times of each T1-weighted non-contrast sequence, total number of non-contrast T1-weighted sequences, and total number of duplicate non-contrast T1-weighted sequences that were repeated.

Image quality data

All data sets were anonymized and stripped of patient identifiers and sequence overlay data. Each of the 62 radial and traditional MRI examinations was provided a study identification and presented in random order to two readers, a radiologist with a certificate of added qualifications (CAQ) in pediatric radiology and 13 years of experience (S.D.B., reader 1), and a pediatric radiology fellow (P.B.D., reader 2). Images were reviewed on a PACS workstation (Synapse; Fujifilm Corporation, Tokyo, Japan). Each reader recorded independent observations with respect to the following image quality parameters on a 5-point Likert scale: overall image quality, hepatic edge sharpness, hepatic vessel clarity and respiratory motion robustness. For each parameter, 1 represented the lowest quality score — unacceptable overall image quality, undetectable parenchymal edge sharpness, unreadable parenchymal vessel clarity and motion artifact degradation — while 5 represented the highest image quality — excellent overall quality, absence of edge and vessel blur, and no motion artifact according to criteria outlined by Ichikawa et al. [15] (Figs. 1 and 2).

Statistical methods

All statistical analyses outlined below were performed using SAS/STAT 14.1 (SAS Institute, Cary, NC) [16]. In particular, the GLIMMIX (generalized linear mixed model) procedure was used for the random effect models (imaging time and image quality assessments), and the IML (interactive matrix language) procedure was used for inter-reader agreement statistics (weighted proportion of agreement and weighted kappa). Tests were two-sided and at the 5% level.

For imaging times (e.g., T1-weighted imaging), the unadjusted treatment effect was the ratio of treatment means for radial and traditional methods. Adjusted treatment effects were based on models including potentially confounding predictors in addition to treatment and, in this case, treatment means and their ratios were evaluated at the means of these predictors. The adjusted model included predictors for gender, age at scan (<10 years, ≥10 years), scanner type (Trio, Skyra, Prisma) and time (years from the first traditional MRI in the study, dated 12 April 2016).

Gamma multiplicative random effect models were used to accommodate the potential correlation between the pair of outcomes from the same subject (one outcome for each method). These are plausible models for correlated and typically right-skewed imaging data [17]. To illustrate using the unadjusted case, with y_{ij} representing imaging time for the i^{th} subject on the j^{th} treatment, the 4-parameter (α, β, v, v_a) random effects model was:

$$y_{ij} \mid a_i \sim gamma\left(exp\left(\alpha + \beta treatment_{ij} + a_i\right), v\right),$$

$$\text{where } a_i \sim normal(0, v_{a.})$$

In this model, the ratio of treatment means is $exp(\beta)$. The random intercept, a_i, specific to the i^{th} subject allows each subject to have their own profile, a profile parallel (on the log scale) to the systematic treatment effect common to all subjects. This random effect is assumed to follow a normal distribution with between-subject variance, v_a, and given the value of a_i, the outcome, y_{ij}, is assumed to follow a gamma distribution with within-subject dispersion, v. The model was estimated by maximizing the approximate integrated likelihood via numerical quadrature.

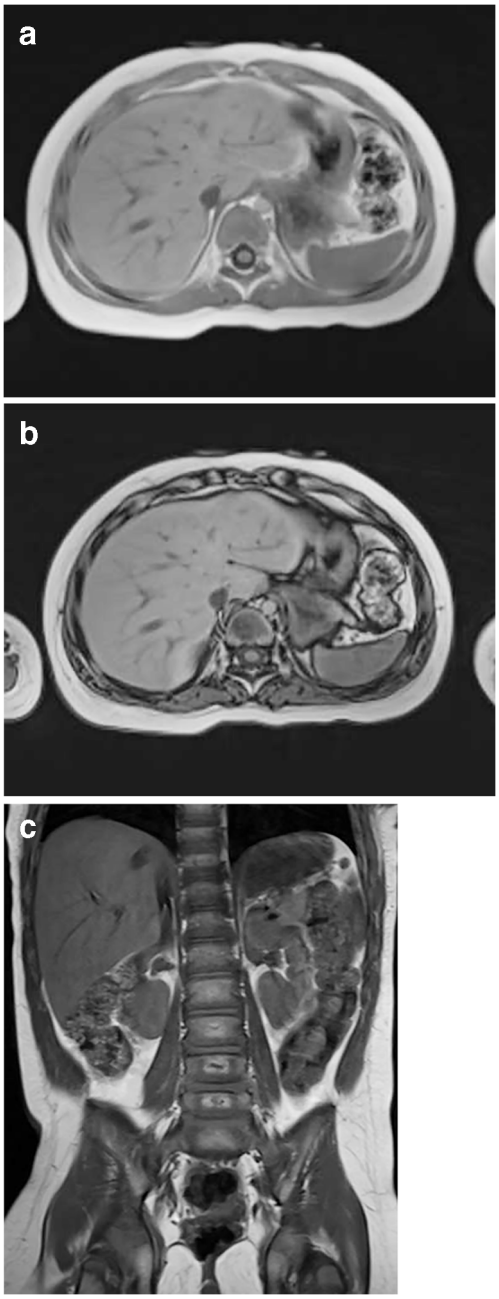

Fig. 2 A 3-year-old girl post resection of a right retroperitoneal neuroblastoma. **a**, **b** In-phase (**a**) and opposed-phase (**b**) images from StarVIBE (volumetric interpolated breathhold examination) Dixon with quality scores of 5 across all metrics by both readers. **c** A traditional study performed 6 months earlier consisted of a coronal T1-weighted turbo spin echo sequence with a mean overall quality score of 3, mean hepatic vessel sharpness score of 3, mean motion robustness score of 3 and mean hepatic edge sharpness score of 3.5

Likert scale image quality assessments (e.g., overall quality) were analyzed in a similar fashion, but using normal linear models rather than gamma multiplicative models. Thus, unadjusted treatment effects were the difference between treatment means for the radial and traditional methods, and adjusted treatment effects were the difference between the treatment means evaluated at the means of gender, age, scanner type and time. The unadjusted normal linear random effects model, in which the difference between treatment means is represented as β, was:

$$y_{ij} \mid a_i \sim normal\left(\alpha + \beta treatment_{ij} + a_i, v\right),$$

$$\text{where } a_i \sim normal(0, v_a)$$

Inter-reader agreement for the four Likert variables was assessed separately for radial (StarVIBE) and traditional methods. Agreement was measured by weighted kappa and the weighted proportion of agreement (weights were based on the squared error metric) [18, 19]. As a guide to interpreting magnitudes for the weighted proportion of agreement (on a scale from 0 to 1), we defined (low, moderate, high) agreement via the ranges (0.5–0.75, 0.75–0.9, 0.9–1). For weighted kappa (on a scale from −1 to 1), these ranges translate to (0–0.5, 0.5–0.8, 0.8–1), which are similar to the recommendations of Fleiss [19]. Our primary measure of agreement was based on the weighted proportion of agreement due to the sometimes erratic behavior and somewhat controversial nature of the kappa statistic [20, 21].

Results

Study population

Thirty-one patients (19 male, 12 female; median age: 5 years; interquartile range: 5 years) comprised the study population. The median length of time between the radial and traditional exams was 242 days (interquartile range: 212 days). Forty-one percent (13/32) of the patients were imaged on the same scanner for both scans, while 59% (19/32) of the patients were scanned on different 3-T scanners. The most common imaging protocol was the abdominal mass protocol (18/31), followed by tuberous sclerosis (7/31), liver mass (3/31), fungemia (2/31) and renal mass (1/31). Diffusion-weighted imaging was performed in 81% (25/31) of the radial exams and 48% (15/31) of the traditional exams. Post-contrast imaging was performed in 90% (28/31) of the radial and 94% (29/31) of the traditional MRI examinations.

Imaging times

Table 2 provides results for the adjusted mean cumulative and component exam times and their radial-versus-traditional ratio for both the full (31 subjects) and BDI (13 subjects) cohorts. Adjusted mean T1-weighted imaging times for the full cohort was 3.63 min (range: 2.0 to 6.6 min) for the radial exams and 8.01 min (range: 2.5 to 18.1 min) for the traditional exams. The ratio of adjusted means for radial (StarVIBE Dixon)

Table 2 Mean imaging time (in min) of radial and traditional exams for the full cohort (31 subjects) and the BDI cohort (13 subjects), adjusted for gender, age, time and scanner

Scan component	All 31 subjects				13 subjects in BDI cohort			
	Radial MRI	Traditional MRI	Ratio of means	*P*-value	Radial MRI	Traditional MRI	Ratio of means	*P*-value
T1-weighted imaging	3.63	8.01	0.45	<0.001	3.98	8.53	0.47	<0.001
Non-T1-weighted non-contrast imaging	28.7	35.5	0.81	0.081	27.7	34.6	0.80	0.094
Non-contrast imaging	32.7	43.9	0.74	0.002	31.9	43.0	0.74	0.003
Post-contrast imaging	33.7	24.7	1.36	0.127	34.8	24.8	1.40	0.284
Total MR imaging	60.2	65.7	0.92	0.387	66.9	71.4	0.94	0.607

BDI indicating the same status for body parts imaged, diffusion-weighted imaging and intravenous contrast administration

versus traditional exams was therefore 0.45 ($P<0.001$). Mean non-contrast imaging times for both exams were 32.7 min versus 43.9 min (ratio: 0.74, $P=0.002$). Similar results were noted for the BDI cohort, with adjusted mean T1-weighted imaging times of 3.98 and 8.53 min for radial and traditional exams (ratio: 0.47, $P<0.001$), and mean non-contrast imaging times of 31.9 and 43.0 min (ratio: 0.74, $P=0.003$).

When T1-weighted imaging was excluded from total non-contrast imaging time, the length of this exam component for the full cohort was 28.7 min for the radial exams and 35.5 min for the traditional exams (ratio: 0.81, $P=0.081$). For the BDI cohort, these times were 27.7 min for the radial exams and 34.6 min for the traditional exams (ratio: 0.80, $P=0.094$).

Adjusted mean total MRI time for the full cohort was 60.2 min for the radial exams and 65.7 min for the traditional exams (ratio: 0.92, $P=0.387$). For the BDI cohort these times were 66.9 min for the radial exams and 71.4 min for the traditional exams (ratio: 0.94, $P=0.607$).

The mean number of non-contrast T1-weighted sequences performed in each radial MRI exam was 1.0 compared to a mean of 1.9 (range: 0–6) for the traditional MRI exams ($P<0.001$). In 29% (9/31) of the traditional exams, the T1-weighted sequence was repeated at least once, and in 13% (4/31) of the patients, more than once.

Image quality assessment

Table 3 provides adjusted mean Likert scores (Likert scale from 1 to 5) for each reader for image quality characteristics for radial and traditional exams for the full cohort (31 subjects). Radial (StarVIBE Dixon) outperformed traditional for all image quality assessments. The radial versus traditional difference in means for reader 1 was 0.84 for overall image quality ($P<0.001$), 0.62 for hepatic edge sharpness ($P=0.006$), 0.88 for hepatic vessel clarity ($P<0.001$) and 1.57 for motion artifact robustness ($P<0.001$). For reader 2, these differences were 0.45 for overall image quality ($P<0.061$), 0.22 for hepatic edge sharpness ($P=0.379$), 0.49 for hepatic vessel clarity ($P<0.041$) and 1.34 for motion artifact robustness ($P<0.001$). Averaging the two readers, these differences were 0.64 for overall image quality ($P<0.001$), 0.42 for hepatic edge sharpness ($P=0.019$), 0.69 for hepatic vessel clarity ($P<0.001$) and 1.49 for motion artifact robustness ($P<0.001$).

Based on the weighted proportion of agreement, inter-reader agreement statistics for (quality, sharpness, clarity, motion) were (0.96, 0.94, 0.90, 0.95) for the radial group (average: 0.94, high agreement) and (0.97, 0.96, 0.93, 0.93) for the traditional group (average: 0.95, high agreement). Based on weighted kappas, the corresponding agreement statistics for (quality, sharpness, clarity, motion) were (0.59, 0.26, −0.21, 0.03) for the radial group (average: 0.16, low agreement), and (0.65, 0.47, 0.32, 0.45) for the traditional group (average: 0.47, low agreement).

Agreement tables for overall image quality are provided in Tables 4 and 5.

Anesthesia data

Airway management decisions were made by the anesthesia team based on patient-specific factors; for example, breath-holding was not required for either radial or traditional MRI protocols. Endotracheal intubation was performed for two patients undergoing radial MRI and three patients undergoing traditional MRI. A laryngeal mask airway was provided for three patients for both radial and traditional MRI. All other patients (26/31 for radial MRI and 25/31 for traditional MRI) underwent imaging with a natural airway.

Discussion

When imaging sedated pediatric patients, the goal is to obtain images as quickly as possible with sufficient resolution to evaluate the targeted structures [2]. Another goal is to

Table 3 Mean adjusted Likert scores for image quality characteristics for radial and traditional exams for the full cohort (31 subjects) adjusted for age, gender, time and scanner

Quality metric	Mean radial MRI		Mean traditional MRI		Difference of means		*P*-value	
	Reader 1	Reader 2	Reader 1	Reader 2	Reader 1	Reader 2	Reader 1	Reader 2
Overall quality	4.14	3.76	3.31	3.31	0.84	0.45	<0.001	0.061
Hepatic edge sharpness	4.08	3.84	3.46	3.62	0.62	0.22	0.006	0.379
Hepatic vessel clarity	3.91	4.05	3.03	3.56	0.88	0.49	<0.001	0.041
Respiratory motion robustness	4.67	4.80	3.10	3.46	1.57	1.34	<0.001	<0.001

minimize the time spent under anesthesia to as low as reasonably achievable (ALARA) given the potential risks associated with anesthesia [22]. The most common indications for patients undergoing abdominal MRI under anesthesia in this study were to evaluate an abdominal mass or to screen patients with tuberous sclerosis. A key requirement for MRI in young patients is to maximize patient cooperation for awake patients, minimize exposure to anesthesia for sedated patients, and reduce scan times in either case. In adults, the ability to breath-hold has enabled rapid GRE sequences to become standard practice in clinical practice over spin-echo sequences for T1-weighted imaging [23]. In children, the limitations around breath-holding have limited the widespread adoption of such fast GRE sequences. Spin-echo imaging with high signal averaging or respiratory triggering has remained standard practice despite lengthy imaging times. The number of signal averages required to perform a single T1-weighted spin-echo sequence (6–8, in our experience) requires an acquisition time between 5 min and 10 min using traditional methods. In more than 40% of the traditional exams in this study, the T1-weighted sequence was repeated at least once, thereby doubling or tripling (or more) the imaging time. in- and opposed-phase imaging or fat-suppressed pre-contrast T1-weighted imaging is also performed, additional imaging time is required.

In this study, we compared performance in terms of imaging time and quality of a free-breathing, radial k-space volumetric GRE Dixon technique in abdominal imaging for sedated pediatric patients to a traditional free-breathing protocol relying on signal averaging or triggering of T1-weighted pulse sequences. Radial imaging is a technique that can be performed during free-breathing whereby k-space sampling occurs via a series of radially-oriented views with net oversampling of the center of k-space and relative undersampling of the periphery. PROPELLER (periodically rotated overlapping parallel lines with enhanced reconstruction) is a hybrid technique between rectilinear and radial sampling [24]. A rectilinear trajectory that samples a "blade" in k-space is rotated around the k-space center to cover a disc in k-space. Fast spin-echo-based PROPELLER sequences are available on major MRI platforms (PROPELLER, Multivane, BLADE) for T2-weighted imaging [4, 25, 26]. The radial technique has been applied to volumetric T1-weighted post-contrast imaging in children and has been shown to achieve superior results compared to conventional Cartesian acquisitions with respect to signal-to-noise ratio and overall image quality [10, 27, 28]. Several investigators have successfully applied 3-D stack-of-stars radial imaging to perform fast, free-breathing liver R_2^* and proton density fat fraction quantification in children and infants [29–32]. Another study investigating free-breathing, non-contrast radial 3-D GRE imaging demonstrated superior performance to a conventional breath-holding counterpart, although this study was in adults without the Dixon technique [8].

In our study population, the mean time spent acquiring T1-weighted imaging before implementing StarVIBE Dixon was more than 8 min (in some instances as long as 18 min). In

Table 4 Inter-reader agreement based on the weighted proportion of agreement and weighted kappa for Likert score image quality characteristics for radial and traditional exams for the full cohort (31 subjects)

Quality metric	Proportion of agreement		Kappa agreement	
	Radial MRI	Traditional MRI	Radial MRI	Traditional MRI
Overall quality	0.96	0.97	0.59	0.65
Hepatic edge sharpness	0.94	0.96	0.26	0.47
Hepatic vessel clarity	0.90	0.93	−0.21	0.32
Respiratory motion robustness	0.95	0.93	0.03	0.45

Table 5 Inter-reader agreement for 5-point Likert scores for overall quality of radial and traditional exams for all 31 subjects

Radial							Traditional						
Frequency	1	2	3	4	5	Total	Frequency	1	2	3	4	5	Total
1	0	0	0	0	0	0	1	0	1	0	0	0	1
2	0	2	0	0	0	2	2	0	5	0	0	0	5
3	0	0	2	1	0	3	3	0	4	9	1	1	15
4	0	0	0	7	1	8	4	0	1	1	6	2	10
5	0	0	3	7	8	18	5	0	0	0	0	0	0
Total	0	2	5	15	9	31	Total	0	11	10	7	3	31

Reader 1: rows; reader 2: columns

contrast, the StarVIBE Dixon was more than twice as fast, with an average imaging time of 3.63 min. Importantly, this was associated with a perceived improvement in image quality. Subjectively measured quality scores were higher for StarVIBE Dixon for each of the four metrics. The most profound improvement in image quality observed by both readers was the respiratory motion robustness of the StarVIBE Dixon sequence. We also demonstrated a reduction in mean non-contrast imaging time. Interestingly, reductions in the length of non-contrast imaging times *outside* of T1-weighted sequences were also noted in the radial exams, which were not attributed to sequence variations or protocol adjustments (Table 2). While this effect did not quite reach statistical significance, it nevertheless suggests that shortening the acquisition time for T1-weighted imaging and removing technical obstacles for the technologists around breath-holding, respiratory gating, and repeat imaging may induce a secondary gain in efficiency with later sequences. If true, this potential improvement in later workflow effects bears further investigation.

All children included in this study were under sedation for their MRI because of their inability to lie still for the duration of an MRI exam while awake due to age or developmental status. A recent study demonstrated that anesthetic exposure in pediatric MRI was positively correlated with MRI scan time, and factors that increase scan time include multiple body part examinations and intravenous contrast administration [33]. Limiting the time spent under anesthesia by performing rapid, high-quality imaging sequences such as StarVIBE rather than lengthier, conventional sequences is in line with efforts to reduce anesthesia exposure. StarVIBE Dixon also eliminates the requirement for breath-holding for T1-weighted imaging, which dramatically changes the depth of anesthesia as well as the need for invasive airway insertion, both of which would decrease both the short-term and long-term risks associated with anesthesia in the MRI setting [34, 35]. At our institution, technical alternatives to breath-holding (triggering, high NSA sequences) are already standard practice for these reasons, at the expense of imaging time.

There are several limitations to this study. Imaging and anesthesia times may have been affected by variations in sequence parameters between the time of the patient's previous MRI (traditional) and study MRI (radial), although there were no formal changes in sequence parameters noted in the protocols. All patients were scanned on 3-T systems with standardized indication-based protocols installed on all scanners. Apart from the introduction of the StarVIBE Dixon sequence, there were no major changes to these protocols during the study period, and an image review confirmed all patients underwent imaging with the same protocol for both the radial and the traditional exams. Readers were not blinded as to which T1-weighted images were being evaluated, which could have introduced bias. This potential bias was minimized by establishing clear and specific evaluation criteria for assessing image quality. As both sets of images were acquired at different imaging episodes separated in time, patient specific factors such as age or growth may have contributed to differences in quality between exams, although we measured, and attempted to adjust for, these in our regression analyses. As the radial exam was always acquired later than the traditional exam, it is possible that patient cooperation improved in the interval between exams.

Conclusion

A free-breathing radial StarVIBE Dixon prototype sequence decreases T1-weighted imaging time in pediatric patients undergoing sedated abdominal MRI with improved image quality when compared to traditional Cartesian T1-weighted sequences. Decreased imaging times and a decreased reliance on breath-holding will create future opportunities for improved patient cooperation and decreased reliance on anesthesia in pediatric patients, areas that warrant further investigation.

Acknowledgments The research reported in this publication was supported in part by the National Institute of Biomedical Imaging and Bioengineering for the National Institutes of Health under award number R01EB019483.

Declarations

Conflict of interests Alto Stemmer works for Siemens Healthineers.

References

1. Chavhan GB, Babyn PS, Vasanawala SS (2013) Abdominal MR imaging in children: motion compensation, sequence optimization, and protocol organization. Radiographics 33:703–719

2. Michael R (2008) Potential of MR-imaging in the paediatric abdomen. Eur J Radiol 68:235–244
3. Vasanawala SS, Iwadate Y, Church DG et al (2010) Navigated abdominal T1-W MRI permits free-breathing image acquisition with less motion artifact. Pediatr Radiol 40:340–344
4. Jaimes C, Kirsch JE, Gee MS (2018) Fast, free-breathing and motion-minimized techniques for pediatric body magnetic resonance imaging. Pediatr Radiol 48:1197–1208
5. Darge K, Anupindi SA, Jaramillo D (2011) MR imaging of the abdomen and pelvis in infants, children, and adolescents. Radiology 261:12–29
6. Rofsky NM, Lee VS, Laub G et al (1999) Abdominal MR imaging with a volumetric interpolated breath-hold examination. Radiology 212:876–884
7. Akisik FM, Sandrasegaran K, Aisen AM et al (2007) Abdominal MR imaging at 3.0 T. Radiographics 27:1433–1444
8. Azevedo RM, de Campos ROP, Ramalho M et al (2011) Free-breathing 3D T1-weighted gradient-echo sequence with radial data sampling in abdominal MRI: preliminary observations. AJR Am J Roentgenol 197:650–657
9. Young PM, Brau AC, Iwadate Y et al (2010) Respiratory navigated free-breathing 3D spoiled gradient-recalled echo sequence for contras-enhanced examination of the liver: diagnostic utility and comparison with free breathing and breath-hold conventional examinations. AJR Am J Roentgenol 195:687–691
10. Chandarana H, Block KT, Rosenkrantz AB et al (2011) Free-breathing radial 3D fat-suppressed T1-weighted gradient echo sequence. Invest Radiol 46:648–653
11. Block KT, Chandarana H, Milla S et al (2014) Towards routine clinical use of radial stack-of-stars 3D gradient-echo sequences for reducing motion sensitivity. J Korean Soc Magn Reson Med 18:87–106
12. Chandarana H, Block KT, Winfield MJ et al (2014) Free-breathing contrast-enhanced T1-weighted gradient-echo imaging with radial k-space sampling for paediatric abdominopelvic MRI. Eur Radiol 24:320–326
13. Balza R, Jaimes C, Risacher S et al (2019) Impact of a fast free-breathing 3T abdominal MRI protocol on improving scan time and image quality for pediatric patients with tuberous sclerosis complex. Pediatr Radiol 49:1788–1797
14. Dixon WT (1984) Simple proton spectroscopic imaging. Radiology 153:189–194
15. Ichikawa S, Motosugi U, Kromrey M-L et al (2020) Utility of stack-of-stars acquisition for hepatobiliary phase imaging without breath-holding. Magn Reson Med Sci 19:99–107
16. SAS Institute Inc (2015) SAS/STAT 14.1 User Guide. SAS Institute, Inc., Cary, NC
17. Fitzmaurice GM, Laird NM, Ware JH (2011) Applied longitudinal analysis, 2nd edn. Wiley, Hoboken, New Jersey
18. Lin L (2012) Statistical tools for measuring agreement. Springer, New York
19. Fleiss J (1981) Statistical methods for rates and proportions, 2nd edn. Wiley, New York
20. Agresti A (2013) Categorical data analysis, 3rd edn. John Wiley & Sons, Hoboken, New Jersey
21. Uebersax J (1987) Diversity of decision-making models and the measurement of interrater agreement. Psychol Bull 101:140–146
22. Callahan MJ, MacDougall RD, Bixby SD et al (2018) Ionizing radiation from computed tomography versus anesthesia for magnetic resonance imaging in infants and children: patient safety considerations. Pediatr Radiol 48:21–30
23. Low RN, Francis IR, Herfkens RJ et al (1993) Fast multiplanar spoiled gradient-recalled imaging of the liver: pulse sequence optimization and comparison with spin-echo MR imaging. AJR Am J Roentgenolog 160:501–509
24. Pipe JG (1999) Motion correction with PROPELLER MRI: application to head motion and free-breathing cardiac imaging. Magn Reson Med 42:963–969
25. Hirokawa Y, Isoda H, Maetani YS et al (2008) MRI artifact reduction and quality improvement in the upper abdomen with PROPELLER and prospective acquisition correction (PACE) technique. AJR Am J Roentgenol 191:1154–1158
26. Bayramoglu S, Kilickesmez O, Cimilli T et al (2010) T2-weighted MRI of the upper abdomen: comparison of four fat-suppressed T2-weighted sequences including PROPELLER (BLADE) technique. Acad Radiol 17:368–374
27. Shin HJ, Kim M-J, Lee M-J, Kim HG (2016) Comparison of image quality between conventional VIBE and radial VIBE in free-breathing paediatric abdominal MRI. Clin Radiol 71:1044–1049
28. Kaltenbach B, Roman A, Polkowski C et al (2017) Free-breathing dynamic liver examination using a radial 3D T1-weighted gradient echo sequence with moderate undersampling for patients with limited breath-holding capacity. Eur J Radiol 86:26–32
29. Zhong X, Hu HH, Armstrong T et al (2020) Free-breathing volumetric liver R 2 * and proton density fat fraction quantification in pediatric patients using stack-of-radial MRI with self-gating motion compensation. J Magn Reson Imaging 53:118–129
30. Armstrong T, Ly KV, Ghahremani S et al (2019) Free-breathing 3-D quantification of infant body composition and hepatic fat using a stack-of-radial magnetic resonance imaging technique. Pediatr Radiol 49:876–888
31. Armstrong T, Ly KV, Murthy S et al (2018) Free-breathing quantification of hepatic fat in healthy children and children with non-alcoholic fatty liver disease using a multi-echo 3-D stack-of-radial MRI technique. Pediatr Radiol 48:941–953
32. Armstrong T, Dregely I, Stemmer A et al (2018) Free-breathing liver fat quantification using a multiecho 3D stack-of-radial technique. Magn Reson Med 79:370–382
33. Machado-Rivas F, Leitman E, Jaimes C et al (2020) Predictors of anesthetic exposure in pediatric MRI. AJR Am J Roentgenol. https://doi.org/10.2214/AJR.20.23601
34. Cravero JP, Blike GT, Beach M et al (2006) Incidence and nature of adverse events during pediatric sedation/anesthesia for procedures outside the operating room: report from the pediatric sedation research consortium. Pediatrics 118:1087–1096
35. Cravero JP, Beach ML, Blike GT et al (2009) The incidence and nature of adverse events during pediatric sedation/anesthesia with propofol for procedures outside the operating room: a report from the pediatric sedation research consortium. Anesth Analg 108:795–804